Chapter 5

Spherical Blastwaves & Supernova Remnants

One way to create a shock is to inject a very large amount of energy into a very small volume. This happens in the interstellar medium whenever a supernova goes off. Suppose an explosion instantaneously injects an amount of energy E into an ambient medium of uniform density ρ_1. The initial energy release is considered to take place within an infinitesimally small volume. Afterward, however, a spherical shock front will expand into the ambient medium. Early in the course of expansion, the pressure within the shock, $P_2 \sim \rho_1 u_{\mathrm{sh}}^2$, is much larger than the ambient pressure P_1 and any radiated energy is much smaller than the explosion energy E. This regime, during which the energy E remains constant, is known as the **blastwave** regime. In a blastwave, the expansion velocity $u_{\mathrm{sh}}(r,t)$, density $\rho(r,t)$, pressure $P(r,t)$, and other properties, are determined solely by the two initial parameters of the system, E and ρ_1.

The energy E has the dimensionality ML^2T^{-2}; the density ρ_1 has the dimensionality ML^{-3}. These two parameters cannot be combined to form a characteristic length scale or time scale for the problem. The solution for the expanding shock front must then be a scale-free or **self-similar** solution. The self-similar solution is a function of the dimensionless variable ξ, where

$$\xi \equiv rt^l \rho_1^m E^n \; ; \tag{5.1}$$

the exponents l, m, and n are determined by the requirement that ξ be dimensionless. Since ξ has the dimensionality $L^{1-3m+2n}T^{l-2n}M^{m+n}$, we see

that the required solution has the exponents $l = -2/5$, $m = 1/5$, and $n = -1/5$, or

$$\xi = r \left(\frac{\rho_1}{Et^2} \right)^{1/5} . \tag{5.2}$$

When expressed in the dimensionless units, the properties of the expanding shock front will depend only on ξ. For instance, the radius of the spherical shock is

$$r_{sh} = \xi_0 \left(\frac{Et^2}{\rho_1} \right)^{1/5} , \tag{5.3}$$

where ξ_0 is a factor of order unity (for $\gamma = 5/3$, it turns out that $\xi_0 = 1.17$). The rate of expansion of the shock is

$$u_{sh} = \frac{2}{5} \xi_0 \left(\frac{E}{\rho_1 t^3} \right)^{1/5} . \tag{5.4}$$

Thus,

$$u_{sh} = \frac{2}{5} \xi_0^{5/2} \left(\frac{E}{\rho_1} \right)^{1/2} r_{sh}^{-3/2} . \tag{5.5}$$

The expanding shock wave slows as it expands. Using typical values for supernova explosions,

$$r_{sh} = 2.3 \, \text{pc} \left(\frac{E}{10^{51} \, \text{erg}} \right)^{1/5} \left(\frac{\rho_1}{10^{-24} \, \text{g cm}^{-3}} \right)^{-1/5} \left(\frac{t}{100 \, \text{yr}} \right)^{2/5} \tag{5.6}$$

$$u_{sh} = 9000 \, \text{km s}^{-1} \left(\frac{E}{10^{51} \, \text{erg}} \right)^{1/5} \left(\frac{\rho_1}{10^{-24} \, \text{g cm}^{-3}} \right)^{-1/5} \left(\frac{t}{100 \, \text{yr}} \right)^{-3/5} \tag{5.7}$$

For instance, SN1054 (which gave birth to the Crab Nebula) should have a radius $r_{sh} \sim 5 \, \text{pc}$ and expansion velocity $u_{sh} \sim 2000 \, \text{km s}^{-1}$, if it is still in the blastwave phase of expansion. In fact, the Crab Nebula is observed to have a radius of $3 \, \text{pc}$ and an expansion velocity of $900 \, \text{km s}^{-1}$. In fact, the Crab is not exactly spherical and its expansion is not exactly energy-conserving, so the discrepancy is not surprising.

Obviously, the self-similar blastwave solution is not good for all times. As $t \to 0$, for instance, the solution predicts infinitely rapid expansion. The self-similar blastwave solution breaks down when the predicted expansion velocity is larger than the velocity with which the supernova initially ejects matter into the ambient medium. For a typical supernova, the initial ejection

velocity is $u_{\rm ej} \sim 10^4 \, \rm km\, s^{-1}$; thus, the blastwave solution is invalid when the supernova remnant is younger than $\sim 70 \, \rm yr$, for our 'standard' supernova parameters.

The self-similar blastwave solution also breaks down when the expanding shock front is very old. The pressure immediately inside the shock is, for an extremely strong shock,

$$P_2 \;\; = \;\; \frac{2}{\gamma + 1} \rho_1 u_{\rm sh}^2 \tag{5.8}$$

$$= \;\; \frac{8}{25} \frac{1}{\gamma + 1} \xi_0^5 E r_{\rm sh}^{-3} \;. \tag{5.9}$$

Thus, the pressure within the blastwave falls off rapidly with radius. If we insert numerical values, we find that

$$r_{\rm sh} \approx 300 \, {\rm pc} \left(\frac{E}{10^{51} \, \rm erg} \right)^{1/3} \left(\frac{P_2}{4 \times 10^{-13} \, \rm dyne\, cm^{-2}} \right)^{-1/3} \;. \tag{5.10}$$

Thus, when a typical supernova remnant reaches a radius of 300 parsecs, the internal pressure has dropped until it is comparable to the ambient pressure of the interstellar medium. This violates our initial assumption that $P_2 \gg P_1$. For our typical supernova remnant, the assumption of negligible pressure breaks down badly at radii of $r_{\rm sh} \sim 300 \, \rm pc$, corresponding to an age of $t \sim 30 \, \rm Myr$.

In finding the blastwave solution, however, we made another assumption; namely, that the energy lost in radiation was small compared to the explosion energy E. At what point does this assumption break down? The temperature within the shock will be, for ionized matter of cosmic abundances,

$$T_2 \;\; = \;\; \frac{2(\gamma - 1)}{(\gamma + 1)^2} \frac{m}{k} u_{\rm sh}^2 \tag{5.11}$$

$$\approx \;\; 2 \times 10^5 \, {\rm K} \left(\frac{m}{10^{-24} \, \rm g} \right) \left(\frac{E}{10^{51} \, \rm erg} \right)^{2/5} \left(\frac{\rho_1}{10^{-24} \, \rm g\, cm^{-3}} \right)^{-2/5} \left(\frac{t}{10^5 \, \rm yr} \right)^{-6/5} \tag{5.12}$$

At an age of $10^5 \, \rm yr$, the radius of the shock will be $r_{\rm sh} \sim 30 \, \rm pc$. The temperature immediately within the shock will be $T_2 \sim 2 \times 10^5 \, \rm K$; the cooling function at this temperature has the value $\rho L \sim 10^{-21} \, \rm erg\, cm^{-3}\, s^{-1}$. The total energy radiated during the course of 10^5 years will be, very roughly,

$$E_{\rm rad} \sim \rho L (\frac{4\pi}{3} r_{\rm sh}^3) t \sim 10^{51} \, \rm erg \;. \tag{5.13}$$

Thus, we expect the energy-conserving blastwave solution to break down because of radiative losses before it breaks down because of pressure equality.

Once radiative losses become significant, a dense shell forms behind the radiative shock. The expanding supernova remnant then passes from its blastwave phase to its **snowplow** phase. Figure 5.1 illustrates the transition from the blastwave phase to the snowplow phase. During the 'snowplow' phase, the matter of the ambient interstellar medium is swept up by the expanding dense shell, just as snow is swept up by a coasting snowplow. During the blastwave phase, energy was conserved; during the snowplow phase, momentum is conserved. Let μ be the total momentum of the expanding shell, so that a region of solid angle $\delta\Omega$ has momentum $\mu\delta\Omega/(4\pi)$. Since the momentum has dimensionality MLT^{-1}, the radius in the self-similar snowplow phase has the dependence

$$r_{\rm sh} = \beta_0 \left(\frac{\mu t}{\rho_1} \right)^{1/4} \; , \tag{5.14}$$

where β_0 is another factor of order unity. The expansion velocity during the snowplow phase is

$$u_{\rm sh} \;\; = \;\; \frac{1}{4}\beta_0 \left(\frac{\mu}{\rho_1} \right)^{1/4} t^{-3/4} \tag{5.15}$$

$$= \;\; \frac{1}{4}\beta_0^{-2} \left(\frac{\mu}{\rho_1} \right) r_{\rm sh}^{-3} \; . \tag{5.16}$$

During the snowplow phase, the momentum of the expanding supernova shell will be of order $\mu \sim M_{\rm sh}u_{\rm sh} \sim 2 \times 10^{43}\,{\rm g\,cm\,s^{-1}}$. The snowplow phase eventually ends when the expansion speed $u_{\rm sh}$ drops to the sound speed $a_1 = (\gamma P_1/\rho_1)^{1/2}$ of the ambient medium. For our typical supernova remnants, this happens at a time $t \sim 2\,{\rm Myr}$, when the radius of the dense shell is $r_{\rm sh} \sim 60\,{\rm pc}$. At this point, the self-similarity of the solution breaks down, since there is now a characteristic length scale $r_c = (E/P_1)^{1/3}$ in the problem. During this last phase of expansion, the shock front degenerates into an acoustic wave, with a velocity of expansion $u_{\rm sh} = a_1$.

So far, we have found the radius of the shock front as a function of time for the blastwave and snowplow solutions. However, we do not yet know the density, velocity, and pressure as a function of radius within the spherical shock front. A solution for ρ, u, and P within a self-similar blastwave was first found by the Russian physicist Leonid Sedov in the 1940's.
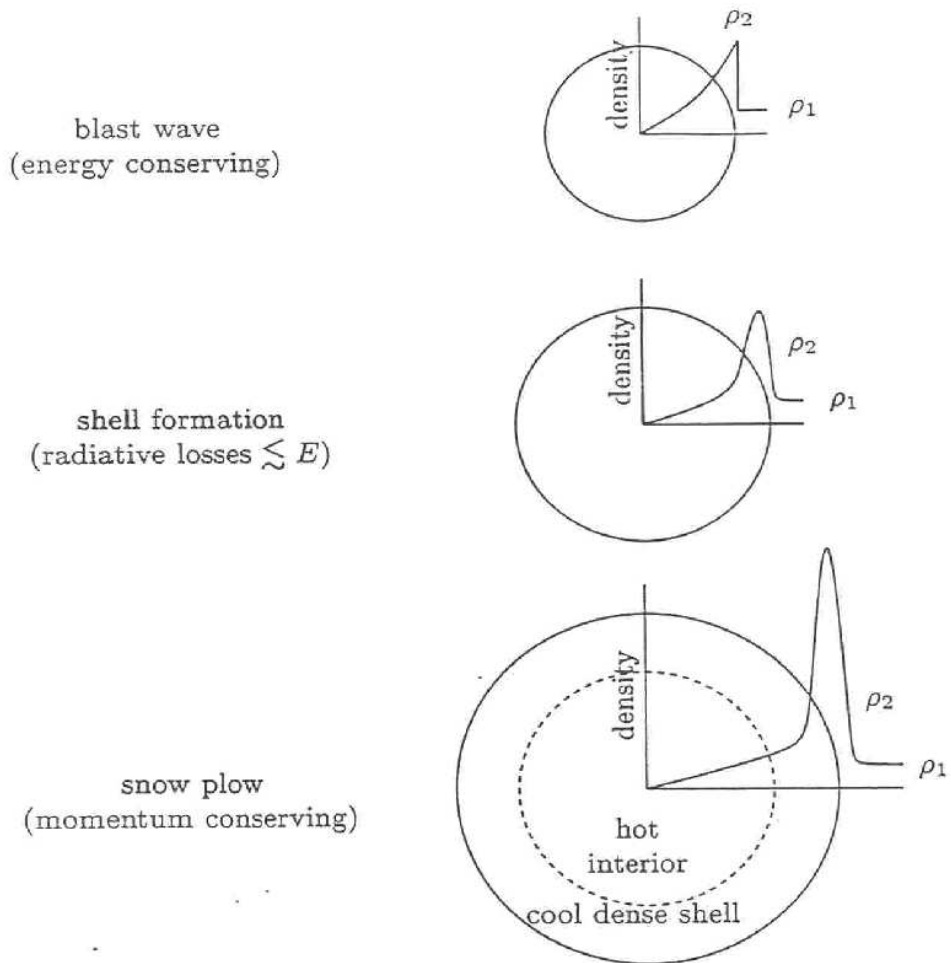
Figure 5.1: An expanding supernova remnant makes the transition from the blastwave phase (upper image) to the snowplow phase (lower image). [Shu, The Physics of Astrophysics, Volume II, Figure 17.4]

The radius of the shock, for the adiabatic blastwave, is $r_{\rm sh} = \xi_o(Et^2/\rho_1)^{1/5}$, and the velocity of expansion is $u_{\rm sh} = (2/5)r_{\rm sh}/t$. If the shock is very strong, the density, bulk velocity and pressure immediately inside the shock front are found from the Rankine-Hugoniot conditions:

$$\rho_2 = \frac{\gamma+1}{\gamma-1}\rho_1 \tag{5.17}$$

$$u_2 = \frac{2}{\gamma+1}u_{\rm sh} \tag{5.18}$$

$$P_2 = \frac{2}{\gamma+1}\rho_1 u_{\rm sh}^2 \ . \tag{5.19}$$

But now, we ask, what are ρ, u, and P for $0 < r < r_{\rm sh}$?

We can find these quantities by solving the equation of mass conservation,

$$\frac{\partial\rho}{\partial t} + \frac{1}{r^2}\frac{\partial}{\partial r}(r^2\rho u) = 0, \tag{5.20}$$

the equation of momentum conservation,

$$\frac{\partial u}{\partial t} + u\frac{\partial u}{\partial r} = -\frac{\partial P}{\partial r} \ , \tag{5.21}$$

and the equation of energy conservation,

$$\frac{\partial}{\partial t}(\rho\varepsilon + \frac{1}{2}\rho u^2) + \frac{1}{r^2}\frac{\partial}{\partial r}[r^2\rho u(\varepsilon + P/\rho + \frac{1}{2}u^2)] = 0 \ , \tag{5.22}$$

where $\varepsilon = P/[(\gamma-1)\rho]$.

Since the solutions for the blastwave is self-similar, the solutions must take the form

$$\rho(r,t) = \left[\frac{\gamma+1}{\gamma-1}\right]\rho_1\alpha(\xi) \tag{5.23}$$

$$u(r,t) = \left[\frac{4}{5(\gamma+1)}\right]\frac{r}{t}v(\xi) \tag{5.24}$$

$$P(r,t) = \left[\frac{8}{25(\gamma+1)}\right]\rho_1\frac{r^2}{t^2}p(\xi) \ . \tag{5.25}$$

The factors of ρ_1, r, and t provide the proper dimensionality for the solutions. The numerical factors in square brackets are inserted so that the dimensionless density, velocity, and pressure have the normalization $\alpha(\xi_0) = v(\xi_0) =$
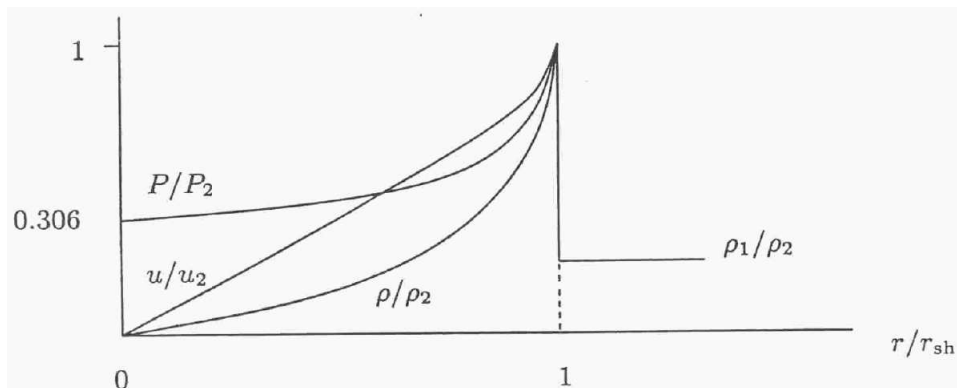
Figure 5.2: The Sedov solution for a spherical blastwave with $\gamma = 5/3$, in units of the immediate post-shock values. [Shu, The Physics of Astrophysics, Volume II, Figure 17.3]

$p(\xi_0) = 1$. The equations of mass, momentum, and energy conservation can now be converted into equations involving the functions $\alpha(\xi)$, $v(\xi)$, and $p(\xi)$. After some numerical manipulation, the mass conservation equation becomes

$$-\xi\frac{d\alpha}{d\xi} + \frac{2}{\gamma + 1}\left[2\alpha v + \xi\frac{d}{d\xi}(\alpha v)\right] = 0 .$$ (5.26)

The momentum conservation equation becomes

$$-v - \frac{2}{5}\xi\frac{dv}{d\xi} + \frac{4}{5(\gamma + 1)}\left[v^2 + v\xi\frac{dv}{d\xi}\right] + \frac{2(\gamma - 1)}{5(\gamma + 1)\alpha}\left[2p + \xi\frac{dp}{d\xi}\right] = 0 .$$ (5.27)

The energy conservation equation, finally, becomes

$$-2(p + \alpha v^2) \;-\; \frac{2}{5}\xi(p + \alpha v^2)$$ (5.28)

$$+ \;\; \frac{4}{5(\gamma + 1)}\left[5v(\gamma p + \alpha v^2) + \xi\frac{d}{d\xi}(v[\gamma p + \alpha v^2])\right] = 0 .$$

Astonishingly, Sedov found an *analytic* solution to these equations. A plot of the solutions is given Figure 5.2. As $\xi \to 0$, the density α and the velocity v go to zero, but the pressure p reaches the limiting value $p = 0.306$ (when $\gamma = 5/3$). This implies that the temperature ($T \propto P/\rho$) goes to infinity as the radius goes to zero.

The time has come to compare our theoretical results with observations of actual supernova remnants (SNRs). Supernova remnants can be observed that correspond to the first three phases of theoretical expansion. The first phase is the **free expansion** of the matter of the exploded star. During this phase, matter moves outward with a constant velocity v_{eject}. The remnant associated with SN1987A is in the free expansion phase. The remnant Cas A is at the end of its free expansion phase; it is ~ 300 years old. At visible wavelengths, many 'knots' of emission, moving radially outward with a velocity of $\sim 6000\,\text{km}\,\text{s}^{-1}$, can be seen. The knots are rich in oxygen, and are interpreted as being clumps of matter that have been ejected from the center of the star, where nucleosynthesis took place.

When the amount of interstellar gas swept up becomes comparable to the initial mass of ejected matter, the SNR enters the blastwave phase. The remnant of Tycho's supernova is in the blastwave phase. The Crab nebula is also in the blastwave phase; its age is $\sim 940\,\text{yr}$, and its expansion velocity is $\sim 900\,\text{km}\,\text{s}^{-1}$.

When the energy radiated just behind the shock front is comparable to the initial energy of the explosion, the SNR enters the snowplow phase. During this phase, a dense cool shell forms directly behind the shock front. In theory, the momentum of this shell is conserved. Observationally, it is found that the internal pressure of SNRs in the snowplow phase is large enough to give a significant push to the shell. The Cygnus Loop (alias the Veil Nebula) is in the snowplow phase; its age is $\sim 4 \times 10^4\,\text{yr}$, and its expansion velocity is $\sim 120\,\text{km}\,\text{s}^{-1}$. The dense shell is thermally unstable to the formation of filaments; such filaments can be seen in optical photographs of the Cygnus Loop.

Although the stages of SNR evolution can be fairly well described by our simple theory, there are many deviations that should be mentioned. First of all, the progenitors of SNRs are massive hot stars that have copious stellar winds. Thus, at the time that the supernova goes off, it will be surrounded by a low-density bubble that has been excavated by the stellar wind. As long as the supernova ejecta are expanding into this low-density region, they will sweep up very little mass, and the free expansion phase will be prolonged. Another complication is that the ambient interstellar medium is not uniform. This inhomogeneity will blur the distinction between the blastwave and snowplow phases; a portion of the shock front that is passing through a dense cloud may be in the snowplow phase, while a neighboring portion that is passing through the rarefied intercloud medium is still in the blastwave

phase.

It should also be noted that massive stars tend to be born in stellar associations. They enter their supernova phase before they have a chance to drift apart. Thus, the remnants of the neighboring supernovas will merge to form a single **superbubble**, which may be hundreds of parsecs across. Such superbubbles are a primary source of the hot ionized component of the interstellar medium.

Chapter 6

Ionization Fronts, HII Regions, & Planetary Nebulae

A shock front is the abrupt transition between two regions with different densities, bulk velocities, and pressures. An **ionization front** is the abrupt transition between a region of ionized gas and a region of neutral gas. The boundary of an **HII region** is an approximation to a spherical ionization front.

An HII region is a volume of photoionized gas surrounding a hot young star (of spectral type O or B). A **planetary nebula** also consists of a volume of ionized gas surrounding a central photoionizing star; the central star in a planetary nebula, however, is an evolved star approaching its death throes. Planetary nebulae tend to be denser and smaller than HII regions. The physics of planetary nebulae is complicated by the fact that the photoionization phase is preceded by the ejection of a large quantity of neutral gas with a velocity of $\sim 20\,\mathrm{km\,s^{-1}}$. Because the structure of an HII region is simpler, I will use it as my basic example of a photoionization region.

The gas in an HII region is ionized by photons emitted by the central star. The ionization energy of hydrogen is $13.6\,\mathrm{eV}$, corresponding to a wavelength of 912 angstroms. To photoionize significant amounts of hydrogen, the stellar temperature must be $T \gtrsim 25{,}000\,\mathrm{K}$. As the star continues to emit photons, the HII region becomes larger. Eventually, enough energy is pumped into the ionized material to raise its temperature and cause it to expand. Thus, a generic HII region consists of a low-density, high-temperature, ionized region expanding outward into the ambient high-density, low-temperature, neutral medium.

The original classic study of HII regions was performed by Bengt Strömgren in 1939. He considered a simple model, which still managed to convey the basic physics of HII regions. We will examine the 'Strömgren sphere', as his model is called, and later examine real HII regions to see how they differ from the ideal case. Strömgren assumed the presence of a uniform medium, consisting of neutral atomic hydrogen, with number density n_0. Suddenly, at time $t = 0$, a hot star turns on at the origin. The star's total output of ionizing photons (in photons per second) is N_u. The initial effect of the star's radiation will be solely to ionize the hydrogen. Thus, the star will be surrounded by a sphere of electrons and protons, with number density $n_e = n_p = n_0$. The spherical volume of ionized gas will be separated from the neutral medium by a thin transition layer, whose thickness is comparable to the mean free path of an ionizing photon in the neutral medium. The mean free path λ_i is given by the relation $\lambda_i = 1/(n_0\sigma_i)$, where the cross-section for photoionization is $\sigma_i \approx 6 \times 10^{-18}\,\mathrm{cm}^2$ for hydrogen atoms.

Initially, the HII region expands outward at a rate given by the relation

$$N_u = n_0 4\pi R^2 \frac{dR}{dt} \ , \tag{6.1}$$

which integrates to

$$R(t) = \left(\frac{3N_u}{4\pi n_0}t\right)^{1/3} \ . \tag{6.2}$$

However, an ionized hydrogen atom does not remain ionized forever. The electrons and protons collide and recombine to form neutral hydrogen at a rate $N_{\mathrm{rec}} = \alpha n_e n_i$. The **recombination rate** $\alpha(T)$ has a value of $\alpha = 2.6 \times 10^{-13}\,\mathrm{cm}^3\,\mathrm{s}^{-1}$ at a temperature $T = 10^4\,\mathrm{K}$, which is a typical temperature for an HII region. Once recombinations become important, the radius of the HII region is given by the relation

$$N_u = 4\pi n_0 R^2 \frac{dR}{dt} + \alpha n_0^2 \frac{4\pi}{3} R^3 \ . \tag{6.3}$$

This has the solution

$$R(t) = R_s \left(1 - e^{-t/t_s}\right)^{1/3} \ , \tag{6.4}$$

where the characteristic time scale is $t_s = 1/(\alpha n_0)$ and the characteristic length scale is the **Strömgren radius**,

$$R_s \equiv \left(\frac{3N_u}{4\pi\alpha n_0^2}\right)^{1/3} \ . \tag{6.5}$$
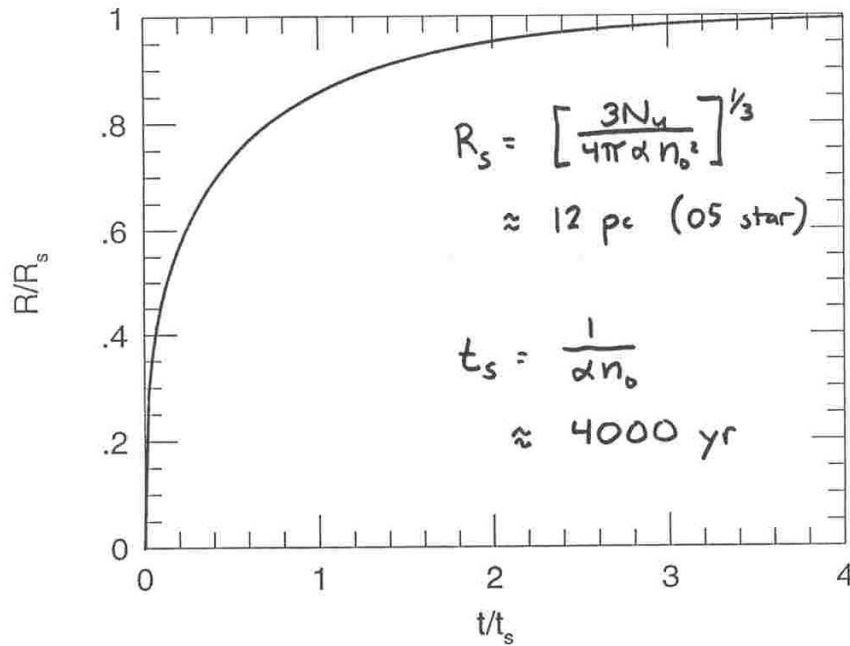
Figure 6.1: The radius of a Strömgren sphere, in units of R_s, as a function of time, in units of t_s.

A plot of the Strömgren sphere's radius as a function of time is given in Figure 6.1. At times $t \gg t_s$, the radius of the HII region will approach the Strömgren radius. An O5 star has $N_u = 5 \times 10^{49}\,\mathrm{s}^{-1}$, and a B0 star has $N_u = 4 \times 10^{46}\,\mathrm{s}^{-1}$. If an O5 star is embedded in a cool neutral cloud with $n_0 = 30\,\mathrm{cm}^{-3}$, it will create an HII region with radius $R_s \sim 4 \times 10^{19}\,\mathrm{cm} \sim 12\,\mathrm{pc}$. The total mass of ionized hydrogen is $\sim 7000\,\mathrm{M_\odot}$. The time to create the Strömgren sphere is $t_s \sim 4000\,\mathrm{yr}$.

The above analysis assumes that the hydrogen gas is static; this is a false assumption. Although the Strömgren sphere is in ionization equilibrium, it is not in dynamic equilibrium. The temperature of the neutral medium in which the HII region will typically be $\sim 100\,\mathrm{K}$. The measured temperatures of HII regions are $\sim 7000\,\mathrm{K}$. Moreover, the HII region has twice as many particles per unit volume as the ambient medium, since its hydrogen is completely ionized into protons and electrons. Thus, the pressure inside the HII region is ~ 140 times the pressure outside. The ionized region will expand outward.

Consider a plane parallel ionization front, across which ρ, P, and u, as

well as the degree of ionization, are discontinuous. Let Φ_i be the flux of ionizing photons reaching the ionization front. Let ρ_1 and P_1 be the density and pressure of the neutral medium, and let u_1 be the bulk velocity of the neutral matter relative to the ionization front. Let ρ_2 and P_2 be the density and pressure of the ionized medium, and let u_2 be the bulk velocity of the ionized matter relative to the front. The continuity equation takes the form

$$\rho_1 u_1 = \rho_2 u_2 = m_i \Phi_i \; , \tag{6.6}$$

where m_i is the mean particle mass of the ionized gas. The momentum conservation equation has the familiar form

$$P_1 + \rho_1 u_1^2 = P_2 + \rho_2 u_2^2 \; . \tag{6.7}$$

The energy equation, however, takes a new and unfamiliar form. Our combination ionization & shock front is radiative, but not isothermal. The temperature T_1 of the neutral medium is constant. The ionized medium is radiatively cooled until it reaches a constant temperature $T_2 \neq T_1$. In a fully ionized medium, the equilibrium temperature that is set by a balance between heating and cooling is generally $T_2 \sim 10^4\,\mathrm{K}$, considerably higher than the temperature $T_1 \sim 100\,\mathrm{K}$ that is typical of the neutral atomic interstellar medium.

In a gas consisting of pure hydrogen, the energy requirements are

$$\frac{P_1}{\rho_1} = \frac{kT_1}{m_H} \tag{6.8}$$

for the neutral gas, and

$$\frac{P_2}{\rho_2} = \frac{2kT_2}{m_H} \tag{6.9}$$

for the ionized gas. We can define the **isothermal sound speeds** for the neutral and ionized media as $a_1 \equiv (P_1/\rho_1)^{1/2}$ and $a_2 \equiv (P_2/\rho_2)^{1/2}$. Making use of the equations for the conservation of mass and momentum, the jump in density across the front can be written in terms of the velocity u_1 and the sound speeds a_1 and a_2. A bit of algebraic manipulation tells us

$$\frac{\rho_2}{\rho_1} = \frac{1}{2a_2^2}[a_1^2 + u_1^2 \pm \sqrt{f(u_1)}] \; , \tag{6.10}$$

where $f(u_1) = (a_1^2 + u_1^2)^2 - 4a_2^2 u_1^2$. The function $f(u_1)$ can also be written in the form

$$f(u_1) = (u_1^2 - u_R^2)(u_1^2 - u_D^2) \tag{6.11}$$

where

$$u_R \equiv a_2 + \sqrt{a_2^2 - a_1^2} \tag{6.12}$$

$$u_D \equiv a_2 - \sqrt{a_2^2 - a_1^2} \;. \tag{6.13}$$

Physical reality demands that the ratio ρ_2/ρ_1 be a real number. Thus, the velocity of the ionization front (relative to the neutral gas) must have either $u_1 \geq u_R$ or $u_1 \leq u_D$. The rapidly propagating ionization fronts $(u_1 \geq u_R)$ are called **R-type fronts**; the slowly propagating ionization fronts $(u_1 \leq u_D)$ are called **D-type fronts**. In this naming scheme, 'R' stands for 'rarefied' and 'D' stands for 'dense'.[1]

In HII regions, it's a fair approximation that $a_2 \gg a_1$, so $u_R \approx 2a_2$ and $u_D \approx (a_1/a_2)^2 a_2/2$. An R-type front always has $u_1 > u_R > a_2 > a_1$, and is supersonic with respect to the neutral medium. A D-type front always has $u_1 < u_D < a_1 < a_2$, and is subsonic with respect to the neutral medium.

For a given propagation velocity u_1, there are two possible values of ρ_2/ρ_1, corresponding to taking the plus or the minus sign in the solution of the quadratic equation. This is shown graphically in Figure 6.2, which is a plot of the ratio ρ_2/ρ_1 as a function of u_1. A front that has the larger density contrast is called a **strong front**; a front that has the smaller density contrast is a **weak front**. Thus, there are four types of ionization front possible; a weak R-type front, a strong R-type front, a weak D-type front, and a strong D-type front. It turns out that strong R-type fronts are unstable, and are not seen in nature. Weak R-type fronts and both strong and weak D-type fronts are known to exist, however, around HII regions and planetary nebulae.

In a weak R-type front, the incoming neutral gas is supersonic with respect to the front $(u_1 > a_1)$, and the outflowing ionized gas is also supersonic with respect to the front $(u_2 > a_2)$. In a strong R-type front, the incoming neutral gas is supersonic, and the outflowing ionized gas is subsonic. In a weak D-type front, the incoming neutral gas is subsonic, and the outflowing ionized gas is also subsonic. In a strong D-type front, the incoming gas is subsonic, and the outflowing ionized gas is supersonic.

Consider, for example, an expanding HII region. When the ionizing star is first 'turned on', the spherical ionization front is very small; hence the flux Φ_i is very large, resulting in a high velocity u_1. Thus, the front is initially

---

[1]For a given flux Φ_i, as the gas becomes more rarefied $(\rho_1 \rightarrow 0)$, the velocity $u_1 \rightarrow \infty$, and an R-type front results. Similarly, as $\rho_1 \rightarrow \infty$, $u_1 \rightarrow 0$, and a D-type front results.
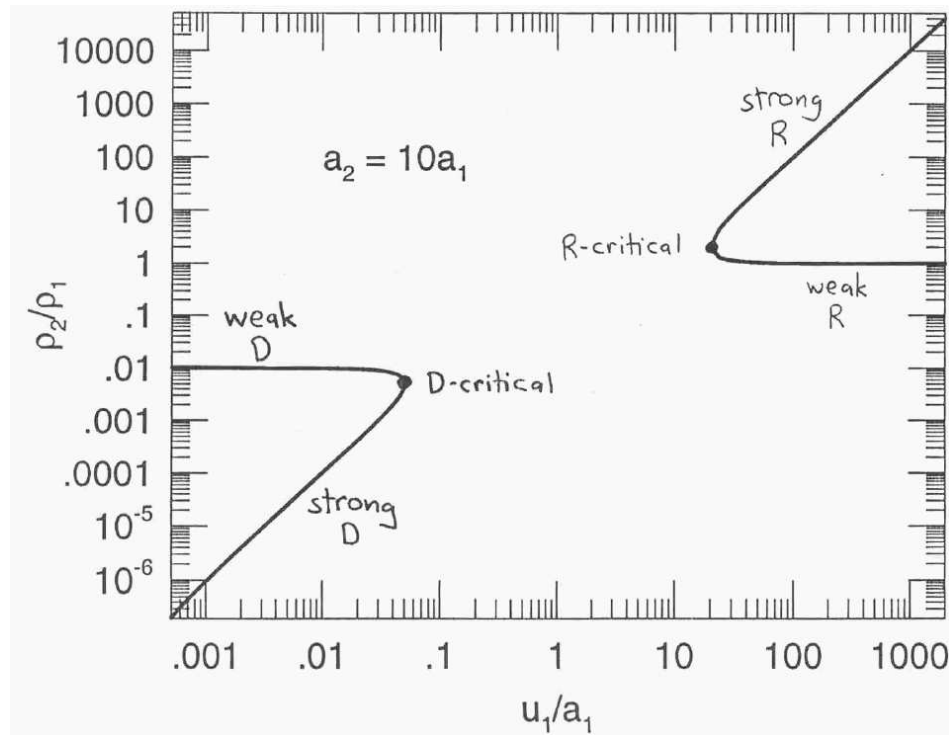
Figure 6.2: Physically permissible values of the density contrast ρ_2/ρ_1 across an ionization front with $a_2 = 10a_1$.

a weak R-type front. In the limit that $u_1 \gg a_2 \gg a_1$, the ratio of densities inside and outside the HII region is

$$\frac{\rho_2}{\rho_1} \approx 1 + \frac{a_2^2}{u_1^2} \qquad \text{weak R .} \tag{6.14}$$

A weak R-type front compresses the gas only slightly. This period, when the interior and exterior densities are nearly the same, is when Strömgren's approximation holds good.

As the ionization front surrounding the HII region expands, the flux of ionizing photons Φ_i steadily decreases. Eventually, the velocity u_1 drops to a value $u_1 = u_R$. At this point, the front is an 'R-critical' front; the density ratio is $\rho_2/\rho_1 \approx 2$ and the velocity of the ionized gas is $u_2 \approx a_2$. Once the ionization front slows still farther, the R-type front can no longer exist. What happens next is illustrated in Figure 6.3. When the velocity u_1 drops below u_R, the R-critical front splits into a shock front followed by a D-critical front. The shock front increases the density of the gas (by a factor of 4 if $M_1 \gg 1$ and $\gamma = 5/3$), decreases the velocity of the gas, and increases the sound speed. Because of the decrease in the bulk velocity and the increase in the sound speed, the flow of neutral gas is now subsonic, and is ready to pass through a D-type front that ionizes it. As the HII region expands farther, the leading shock front gradually weakens, and the trailing D-critical front develops into a weak D-type front. Thus, a bit of neutral gas will be first compressed by the shock and then blasted with UV photons and ionized.

The shock front expands outward and decreases in amplitude until it finally becomes a sound wave of infinitesimal amplitude expanding outward with velocity $u_1 = a_1$. If the photoionizing star is immortal, then the ionization front will expand more and more slowly until HII region attains an equilibrium state in which the pressure of the expanded ionized gas is equal to the pressure of the neutral surrounding medium. The final equilibrium radius, R_{final}, is given by the relation

$$R_{\text{final}} = \left(\frac{3N_u}{4\pi\alpha n_{\text{final}}^2} \right)^{1/3} , \tag{6.15}$$

where the density n_{final} within the HII region is given by the requirement of pressure equilibrium:

$$2n_{\text{final}}T_2 = n_0 T_1 . \tag{6.16}$$

Before transition

$\rho = \rho_1$ $\rho \approx 2\rho_1$

$\longrightarrow$ $\longrightarrow$

$u_1 \approx u_R \approx 2a_2$ $u_2 \approx a_2$

neutral   ionized

weak R
ionization front

- -

After Transition

$\rho = \rho_1$ $\rho \approx 400\rho_1$ $\rho \approx 2\rho_1$

$\longrightarrow$ $\overset{\rightarrow}{u \approx \frac{1}{200} a_2}$ $\longrightarrow$

$u_1 \approx 2a_2$ $u_2 \approx a_2$

neutral   neutral   ionized

Radiative   weak D
Shock   ionization
                            front
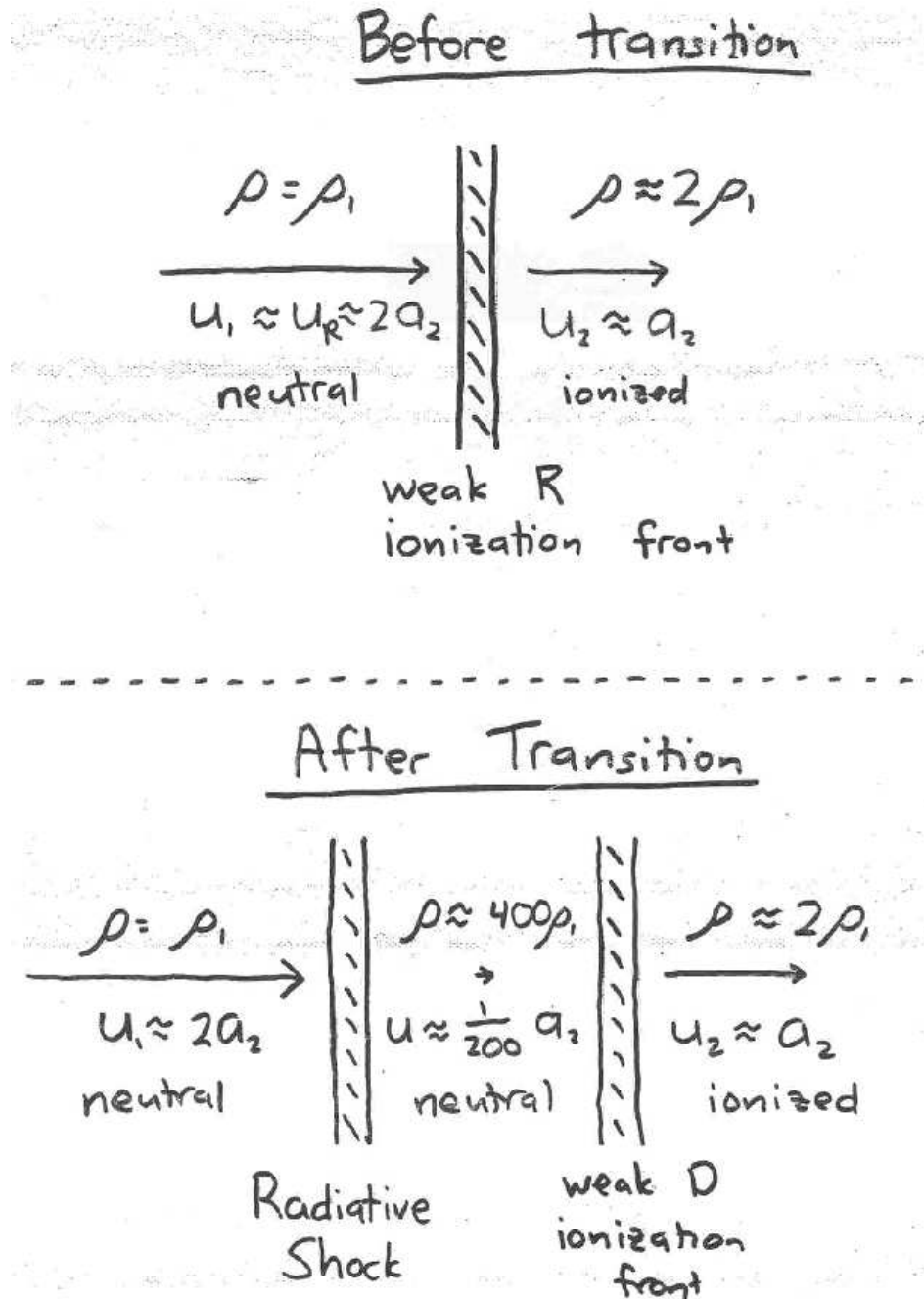
Figure 6.3: The transition from an R-critical front to a shock front followed by a D-critical front.

Thus,

$$R_{\text{final}} = \left(\frac{2T_2}{T_1}\right)^{2/3} R_s \sim 27 R_s \ . \tag{6.17}$$

In practice, however, HII regions never reach this equilibrium state. The massive O and B stars that ionize them become supernovae before then.

Observers classify real HII regions into five categories that correlate well with the age of the region. An **ultracompact** HII region contains a single, very young, hot star. Ultracompact HII regions are embedded deep within molecular clouds, and can be observed only in the radio and the infrared. They have radii $R \lesssim 0.1 \, \text{pc}$ and densities $n \gtrsim 10^4 \, \text{cm}^{-3}$. An example of an ultracompact HII region is the Becklin-Neugebauer object, located in a molecular cloud near the Orion nebula.

As the HII region expands, it becomes a **compact** HII region. A compact HII region contains a single, young, hot star; it has broken out of its molecular cocoon, so it can be seen at optical wavelengths. Compact HII regions have radii $R \sim 0.5 \, \text{pc}$ and densities $n \sim 5 \times 10^3 \, \text{cm}^{-3}$. An example of a compact HII region is the Orion nebula.

A **standard** HII region contains a single hot star; it typically forms a 'blister' on the surface of a molecular cloud. On one side, the expanding ionized gas of the HII region is confined by the dense molecular cloud; on the other side, it pushes out into the intercloud medium. Standard HII regions have $R \sim 3 \, \text{pc}$ and $n \sim 300 \, \text{cm}^{-3}$. An example of a standard HII region is the Omega nebula.

A **large** HII region contains several hot stars; it consists of several standard HII regions that have merged together. Large HII regions have $R \sim 10 \, \text{pc}$ and $n \sim 50 \, \text{cm}^{-3}$. An example of a large HII region is the North America nebula.

Finally, a **giant** HII region contains as many as 10^4 hot stars; it consists of numerous large HII regions plus a common ionized envelope. Giant HII regions have $R \gtrsim 100 \, \text{pc}$ and $n \lesssim 10 \, \text{cm}^{-3}$. A famous example of a giant HII region is 30 Doradus in the Large Magellanic Cloud.

Planetary nebulae contain one hot star apiece, but they show an increasing radius and decreasing density similar to that of HII regions. The youngest visible planetary nebulae have $R \sim 0.03 \, \text{pc}$ and $n \sim 10^4 \, \text{cm}^{-3}$. The oldest planetary nebulae have $R \sim 1 \, \text{pc}$ and $n \sim 10 \, \text{cm}^{-3}$. The progenitor of a planetary nebula is a star of initial mass $1 - 8 \, \text{M}_\odot$ that has evolved onto the asymptotic giant branch (AGB). At the end of its AGB stage, such a star
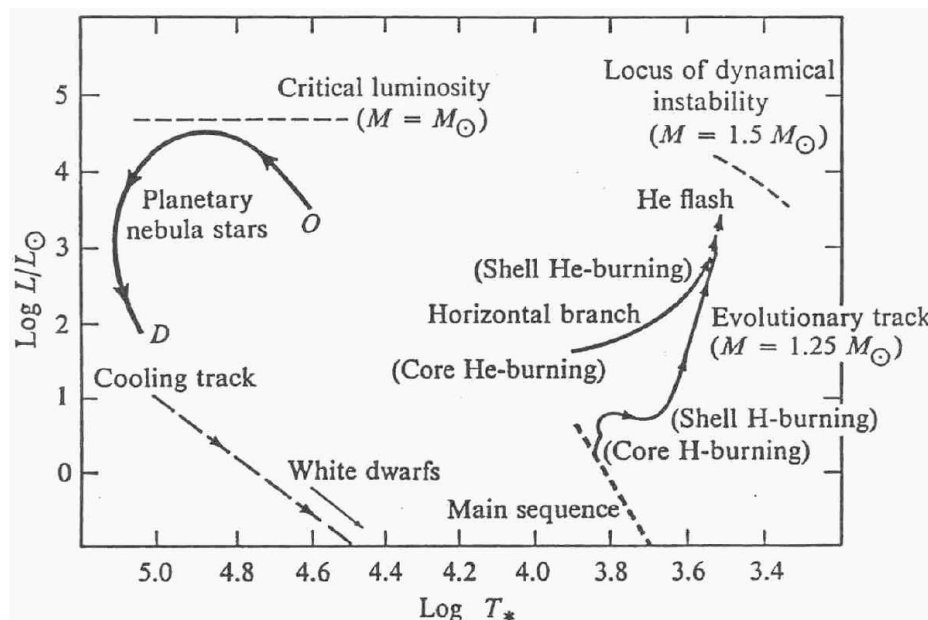
Figure 6.4: A schematic luminosity – temperature diagram for the evolution of stars destined to become planetary nebulae.

ejects its outer envelope at the relatively low velocity of $20 - 30 \, \mathrm{km \, s^{-1}}$. A central core of mass $0.6 - 1.4 \, \mathrm{M_\odot}$ is left behind. This central core, which evolves into a white dwarf, is the photoionization source for the planetary nebula. The evolution of the central stars of planetary nebulae is given in Figure 6.4.

The central photoionizing core has a temperature of $25{,}000 \, \mathrm{K} \to 200{,}000 \, \mathrm{K}$, and a luminosity $10 \, \mathrm{L_\odot} \to 10{,}000 \, \mathrm{L_\odot}$. The ejected matter that is photoionized by the central core is initially cold and neutral, and consists partly of molecules. (Thus, the ionization front in a planetary nebula is preceded by a **dissociation front**.) Initially, the ionized matter surrounding the central core consists entirely of the matter that has been ejected from the giant progenitor. However, as the ionization front expands, it reaches the boundary of the ejected matter, and reaches the lower-density interstellar matter beyond. The ionization front races outward into the low-density surrounding matter. Eventually, however, the temperature of the central white dwarf drops below $25{,}000 \, \mathrm{K}$ and fails to maintain the ionization of the surrounding matter. The planetary nebula gradually recombines, and dims into invisibility.